J Appl Electrochem (2011) 41:1367–1371
DOI 10.1007/s10800-011-0337-5

SHORT COMMUNICATION

Localized CO_2 corrosion propagation at moderate $FeCO_3$ supersaturation initiated by mechanical removal of corrosion scale

Jiabin Han · J. William Carey

Received: 28 March 2011 / Accepted: 10 July 2011 / Published online: 24 July 2011

Abstract The propagation of localized CO_2 corrosion was investigated at moderate iron carbonate supersaturation using an artificial defect method with re-formed corrosion scale. A mechanical tool was developed which locally removed pre-formed iron carbonate scale and initiated localized corrosion at a $FeCO_3$ supersaturation of 3–10. The localized corrosion rate was calculated based on electrochemical measurement using a simplified algorithm and was also measured at the deepest part of the defect using scanning electron microscopy. Localized corrosion was driven by a galvanic cell established between the two surfaces exposed in the artificial defect where an open circuit potential difference was maintained.

Keywords Localized corrosion · Carbon dioxide · Electrochemistry · Scale

1 Introduction

Field experience of CO_2 corrosion shows that infrastructure can fail within a few years, even months, which is a much shorter lifetime than the typical 30–50 year design-life (which is based on uniform corrosion models). Most failures are caused by localized CO_2 corrosion [1]. In general, when a pipeline or production casing is exposed to an aqueous fluid containing CO_2, an iron carbonate scale forms on the steel wall where the fluid exceeds supersaturation conditions. Damage of this scale, mechanically or chemically, results in locally accelerated corrosion. These processes are affected by interrelated factors including flow (causing flow-induced localized corrosion) [2, 3], $FeCO_3$ supersaturation [4, 5], pH [5, 6], anions/cations [7, 8], temperature [4], scale properties [9, 10], and metallurgy [11, 12]. Recent research by Han et al. [5, 13] clarified the galvanic mechanism of localized CO_2 corrosion. Two surfaces with and without scale were studied; a different open circuit potential measured across the surfaces established the existence of a galvanic cell. The corrosion process was accelerated tens of times due to balancing of the mixed potential between these two surfaces. In these articles, a worst-case scenario was investigated assuming localized corrosion proceeded at a rate corresponding to a freshly developed, bare pit anode where the galvanic cell held maximum galvanic potential difference. Steady localized corrosion continued at small degrees of $FeCO_3$ supersaturation of 0.5–2 [5, 13]. In this study, we investigate localized corrosion at moderate levels of $FeCO_3$ supersaturation and hypothesize that a porous corrosion scale forms in the pitted surface, resulting in a reduced rate of localized corrosion, but that does not stop localized corrosion. This is a more realistic condition for field conditions and could be used to estimate long term localized corrosion propagation.

In order to investigate the hypothesized scenario, a mechanical film removal technique was developed to artificially initiate localized corrosion. In this study, an $FeCO_3$ film is formed at initially high $FeCO_3$ supersaturation (SS_{FeCO_3}) > 300 and allowed to reach steady state. Then a small region of the protective iron carbonate scale was mechanically removed, initiating localized corrosion. Then the evolution of the induced localized corrosion rate was followed as a function of the aqueous solution supersaturation of $FeCO_3$.

J. Han (✉) · J. William Carey
Earth and Environmental Sciences Division,
Los Alamos National Laboratory, Los Alamos, NM 87545, USA
e-mail: jhan@lanl.gov; jiabin.han@gmail.com

2 Experimental design and procedure

A scratch tool was designed to locally remove a pre-formed protective ferrous carbonate scale and initiate localized corrosion (Fig. 1). It consisted of a stainless steel blade with width of 2 mm and hardness similar to that of mild steel. This blade removed only the softer iron carbonate scale while not damaging the harder steel substrate beneath the scale. The tool was operated by touching the blade to an $FeCO_3$-covered cylindrical electrode rotating at 300 rpm. This created a fresh steel surface which acted as an anode with respect to the scale-covered surface which served as a cathode. This geometry simulated a "mesa" type of localized corrosion typically observed in oil and gas pipelines [5].

A three-electrode electrochemical glass cell was used for the corrosion measurements. The working electrode was a C1018 mild steel rotating cylindrical electrode (RCE). All the potentials were measured and reported versus an Ag/AgCl reference electrode filled with a 4 M KCl electrolyte. The reference electrode was connected to the experimental solution via a Luggin capillary salt bridge capped by a porous Vycor tip and filled with 1 mol L^{-1} of KCl.

The glass cell was filled with 2 L of 1 wt% NaCl electrolyte, heated to 80 °C and deaerated by purging with CO_2 throughout the experiment. The pH of the solution was adjusted to 6.6 by slowly injecting 1 mol L^{-1} $NaHCO_3$ solution. CO_2 was then purged for one additional hour before starting the experiment.

The RCE (outer exposed surface area 5.4 cm^2) was prepared by polishing with 200, 400, and 600-grit sandpaper sequentially. The surface was cooled by spraying 2-propanol during grinding. It was then flushed and ultrasonicated with 2-propanol and blown dry with air. A protective $FeCO_3$ scale was deposited on the RCE as follows: An $FeCl_2$ solution was deaerated in a beaker covered with a plastic film. A syringe was deaerated by purging with CO_2 for at least five cycles of the syringe plunger. The syringe was used to transport a calculated amount of deaerated $FeCl_2$ solution and the solution was slowly injected into the glass cell to achieve an initial 50 ppm Fe^{2+} concentration or initial supersaturation (SS_{FeCO_3}) of 392. The solution was well mixed to avoid locally high supersaturation and undesired rapid nucleation of $FeCO_3$. The resulting solution yielded evenly precipitated $FeCO_3$ scale on the RCE. With time, Fe^{2+} was consumed by the formation of $FeCO_3$ scale and its concentration, periodically measured using a spectrophotometer, dropped to less than 3 ppm after 24 h. Then a small region of the corrosion scale was removed to create a bare surface by pressing the scratch tool against the RCE for 2 min, which initiated localized corrosion. As iron accumulated in the solution from renewed corrosion, scale reformed on the scratched surface. Periodically, the RCE was re-scratched at exactly the same place.

During the experiment, the pH was adjusted periodically by the addition of dilute HCl solution (pH $\approx$ 2; deaerated using the previously described procedure for $FeCl_2$) to control the iron carbonate supersaturation to a moderate level of 3–10 (Table 1). The iron carbonate supersaturation was calculated by an aqueous speciation solubility model based on the measured iron concentration and pH at a CO_2 pressure of 0.53 bar (thermodynamic values for iron carbonate given in [14]; the aqueous speciation model is described in [15]). The corrosion resistance was measured based on the area of the scratched and intact surfaces using linear polarization resistance (LPR) and electrochemical

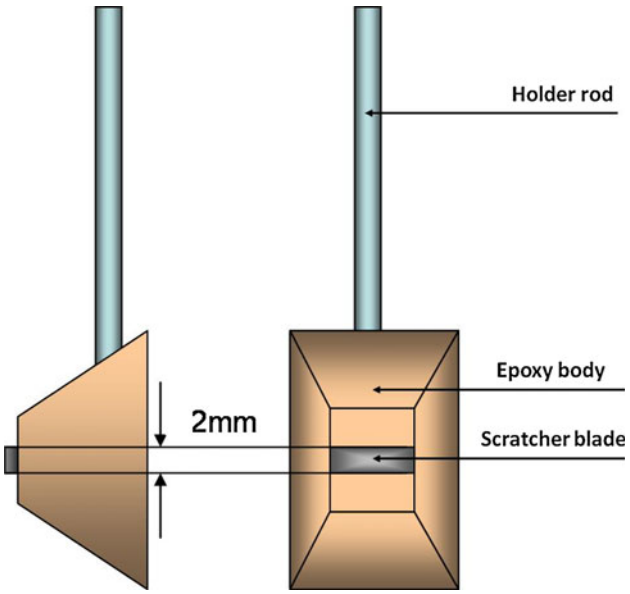

Fig. 1 Schematic diagram of the scale scratcher

Table 1 Calculated iron carbonate supersaturation at conditions during experiments

Time/h	$[Fe^{2+}]$/ppm	pH	SS_{FeCO_3}
0	1.5	6.57	10.7
0.48	1.5	6.30	3.3
24.41	3.5	6.25	5.6
25.65	3.5	6.12	3.1
50.55	9.2	6.16	10.1
50.78	9.2	5.92	3.4
51.22	9.2	5.90	3.0
119.9	17.6	5.95	7.3
120.0	17.6	5.76	3.1
143.7	25.7	5.82	5.9
143.7	25.7	5.71	3.6
162.3	26.8	5.77	4.7

Table 2 Test parameters for corrosion experiments

Material	C1018 mild steel
RCE outer surface area/cm^2	5.4
RCE length/cm	1.4
Scratched ring width/cm	0.2
Ratio of un-scratched/scratched surface	7
Solution volume/L	2.0
Temperature/°C	80
pH	6.6 → 5.7
pCO_2/bar	0.53
NaCl concentration/wt%	1.0
RCE rotating speed/rpm	0
Solution stirring	Stirred
Electrochemical measurements	LPR, EIS
Analysis	SEM
LPR	
Polarization potential/mV versus OCP	±5.0
Scan rate/mV s^{-1}	0.2
EIS	
Frequency range/Hz	0.01–100,000
Peak to peak amplitude/mV versus OCP	20

impedance spectroscopy (EIS). The electrochemical measurement parameters and test conditions are summarized in Table 2. Uniform corrosion and localized corrosion rates were calculated using a simplified algorithm described in the following section. A cross section through the localized corrosion region was analyzed using scanning electron microscopy (SEM).

3 Results and discussion

In CO_2 brine systems, the equilibrium reactions including solubility and speciation of CO_2, water dissociation, and $FeCO_3$ formation are as follows [15]:

$$CO_{2(g)} \xleftrightarrow{K_{H,CO_2}} CO_{2(aq)} \quad (1)$$

$$CO_{2(aq)} + H_2O_{(aq)} \xleftrightarrow{K^O_{0,CO_2}} H_2CO_{3(aq)} \quad (2)$$

$$H_2CO_{3(aq)} \xleftrightarrow{K^O_{1,CO_2}} H^+_{(aq)} + HCO^-_{3(aq)} \quad (3)$$

$$HCO^-_{3(aq)} \xleftrightarrow{K^O_{2,CO_2}} H^+_{(aq)} + CO^{2-}_{3(aq)} \quad (4)$$

$$H_2O_{(aq)} \xleftrightarrow{K^O_w} H^+_{(aq)} + OH^-_{(aq)} \quad (5)$$

$$Fe^{2+}_{(aq)} + CO^{2-}_{3\,(aq)} \xleftrightarrow{K^O_{sp,FeCO_3}} FeCO_{3(s)} \quad (6)$$

The electrochemical reactions include anodic and cathodic half-cell reactions: reduction of carbonic acid, protons, bicarbonate and water and oxidation of iron [15]:

$$2H_2CO_{3\,(aq)} + 2e^- \rightarrow H_{2\,(g)} + 2HCO_3{}^-{}_{(aq)} \quad (7)$$

$$2H^+{}_{(aq)} + 2e^- \rightarrow H_{2\,(g)} \quad (8)$$

$$2H_2O\,(l) + 2e^- \rightarrow H_{2\,(g)} + 2OH^-{}_{(aq)} \quad (9)$$

$$Fe_{\,(s)} \rightarrow Fe^{2+}{}_{(aq)} + 2e^- \quad (10)$$

The overall corrosion reaction is:

$$H_2CO_{3\,(aq)} + Fe \rightarrow FeCO_{3\,(aq\ or\ s)} + 2H_2\,(g) \quad (11)$$

3.1 Localized corrosion rate calculation using electrochemical measurements

3.1.1 Simplified algorithm to calculate localized corrosion rate

Three assumptions were made to simplify the calculation of localized corrosion rate using the electrochemical measurements. First, the uniform corrosion rates on a bare carbon steel surface are assumed to be constant between pH 5.0 and 6.6. At this pH range, the dominant cathodic reaction is carbonic acid reduction, and the proton reduction contribution to corrosion is negligible (<5%) [15]. The observed difference of uniform corrosion rates between pH 5.0 and 6.6 is less than 10% [16], which is within the error of electrochemical measurements. Second, the protectivity of the iron carbonate scale is assumed to be constant at pH 5.0–6.6 as long as iron carbonate is supersaturated. Last, localized corrosion is initiated immediately after the film is scratched.

At the mixed potential, equal to the measured open circuit potential (OCP) of the total scratched and un-scratched sample surfaces, the corrosion currents (I_{corr}) measured by LPR and EIS are equal to the anodic currents ($I_{a,t}$) or the cathodic currents ($I_{c,t}$) on both scratched and scale-covered surfaces. The sum of the currents is zero, obeying the neutral charge law.

Anodic currents $I_{a,t}$ include those from the scratched surface (I_s) and the scale-covered surface (I_f):

$$I_{a,t} = I_s + I_f \quad (12)$$

In terms of current density:

$$i_t \times A_t = (i_s \times A_s) + (i_f \times A_f) \quad (13)$$

where i_t is the total current density, A m^{-2}; A_t is the total area, m^2, 0.054 m^2 in this study; i_s is the current density from the scratched area, A m^{-2}; A_s is the exposed scratched area, m^2, 0.0077 m^2 in this study; i_f is the current density from the scale-covered area, A m^{-2}; A_f is the area covered by the protective scale, m^2.

The ratio of the total area to the scratched area in this study is:

$$r = A_t/A_s = 7 \quad (14)$$

The corrosion rate is linearly related to the corrosion current density [17]:

$$CR = 1.155 \times i \quad (15)$$

where CR is the corrosion rate, mm year^{-1} and i is the corrosion current density, A m^{-2}.

Substituting Eqs. 13–15 into Eq. 12, the corrosion rate for the scratched area can be determined:

$$CR_s = CR_t \times r - CR_f \times (r - 1) \quad (16)$$

where CR_s is the corrosion rate of the scratched area (i.e., the localized corrosion rate), CR_t is the corrosion rate measured with the scratch at the mixed potential, and CR_f is the corrosion rate on the scale-covered surface measured before the scratch.

3.1.2 Localized corrosion propagation observations

During scale formation (Fig. 2), the corrosion rate of the initially fresh steel surface was 1.2 mm year^{-1}. It decreased and stabilized at about 0.2 mm year^{-1} (CR_f). The corrosion potential started to increase after 10 h as the iron carbonate scale continued to form. This phenomenon agrees with previous reports, possibly due to the formation of a pseudo-passive film [5, 13].

The scale was scratched after 1 day of immersion and scale formation after a stable corrosion potential was achieved. Localized CO_2 corrosion measurements were initiated immediately. The mixed potential decreased ca. 10 mV in less than 2 min (Fig. 3) indicating that the potential on the scale-covered surface was higher than that on the newly scratched surface. This rapid change in potential is consistent with the establishment of a galvanic cell between the two surfaces [5, 13].

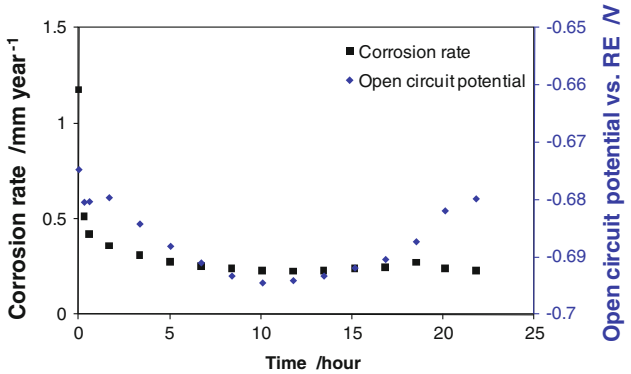

Fig. 2 History of uniform corrosion rate and open circuit potential during scale formation before the scratch

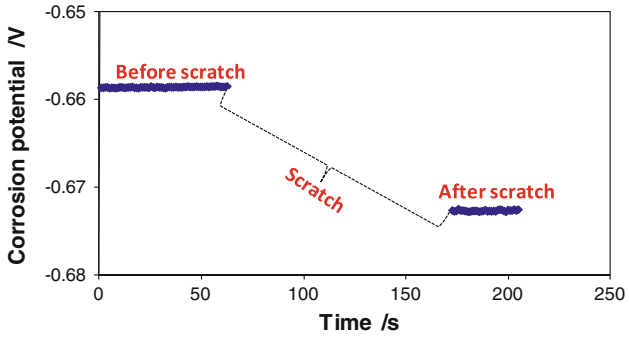

Fig. 3 An example experiment showing the change in open circuit potential following the scratch of the surface

The localized corrosion rate increased sharply (Fig. 4) after each scratch. In scratch 2–5, a decrease in corrosion rate was observed, consistent with the steady re-formation of scale. The behavior of scratch 1 was more complex but may reflect incomplete removal of scale by the scratch tool or some other transient phenomena. The time averaged localized corrosion rate on the scratched surface was 3.7 mm year^{-1}, a higher corrosion rate compared with the bare surface corrosion rate (1.2 mm year^{-1}), and much higher than the uniform corrosion rate (0.2 mm year^{-1}) of the scale-covered surface without a scratch. Thus, the pit surface corrosion rate was accelerated due to positive polarization (galvanic effect) induced by the scale-bearing surface. It is noted that the observed localized corrosion rate in the presence of re-formed scale was lower than the localized corrosion rate observed in a bare pit of 10-20 mm year^{-1} [5].

3.2 Localized corrosion rate measurement using SEM

A SEM cross section image of the scratched area shows that the surrounding surface was covered by a 12-μm compact iron carbonate scale (Fig. 5). The uniform corrosion rate measured by the depth of corrosion in the SEM

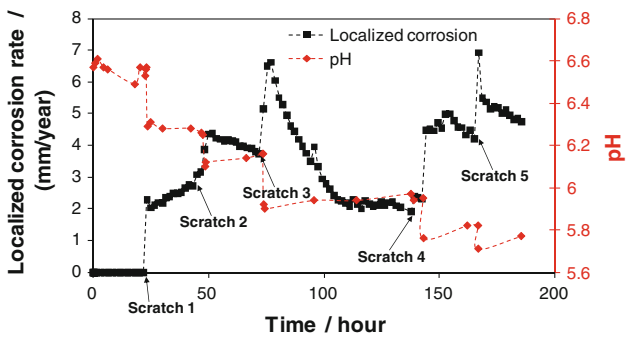

Fig. 4 History of localized corrosion rate during repeated scratching of the $FeCO_3$ scale together with measured pH

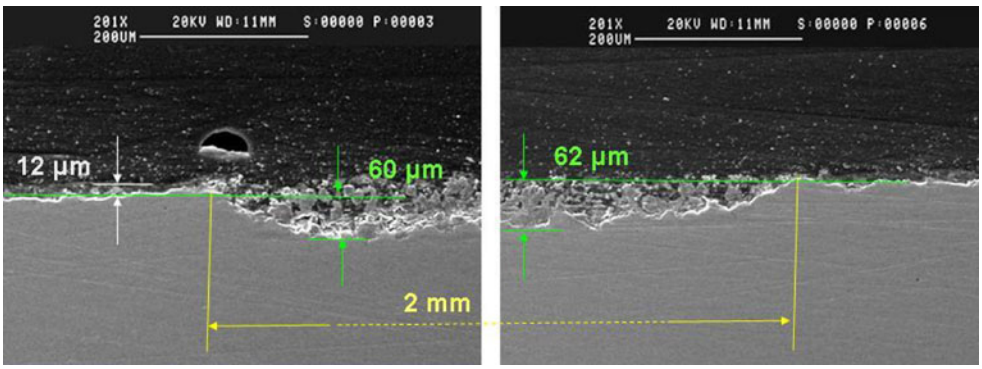

Fig. 5 SEM images of a cross section through the region of localized corrosion formed by scratching the $FeCO_3$ scale

image is equal to 0.57 mm year^{-1}. This agrees with the time averaged corrosion rate (0.65 mm year^{-1}) measured using electrochemical methods. The localized corrosion depth was measured at 60–63 µm after 160 h of exposure. This mesa surface was filled with a porous scale. The time averaged localized corrosion rate is 3.5 mm year^{-1}. The measured depth provides a relatively accurate measure of the localized corrosion rate because the scratch technique produces a relatively uniform and flat-bottomed defect (Fig. 5). The measured data agrees with the above calculated localized corrosion rate using electrochemical data (3.7 mm year^{-1}).

4 Conclusions

Localized CO_2 corrosion was initiated at moderate $FeCO_3$ supersaturation (3–10) by locally removing a pre-formed iron carbonate scale. The localized corrosion rates were calculated at 3.7 mm year^{-1} using electrochemical techniques and were measured at 3.5 mm year^{-1} based on the depth observed by SEM of a cross section through the surface. The mixed potential decreased as a new fresh surface was created from the scaled surface, which underpins the galvanic mechanism of localized corrosion. A scenario of localized CO_2 corrosion propagation was observed: a propagating pit filled with a partially protective iron carbonate scale at moderate supersaturation.

Acknowledgments The authors thank the Fossil Energy program of DOE for grant FE-10-001-FY11. The author, Jiabin Han, would like to acknowledge the financial support to allow the experimental work from the Joint Industry Project advisory board members of Institute for Corrosion and Multiphase Technology of Ohio University: Baker Hughes, BG Group, BP, Champion, Chevron, Clariant, Conoco Phillips, Encana, Eni, ExxonMobil, INPEX, IONIK, MI-Swaco, Nalco, Occidental Oil, Petronas, Petrobras, PTTEP, Saudi Aramco, Shell, Tenaris and Total.

References

1. Kane RD, Eden DA, Eden DC (2003) In: Proceedings of NACE CORROSION/2003, no. 03175
2. Schmitt G, Bucken W, Fanebust R (1991) Corrosion 48:431
3. Schmitt G, Bosch C, Pankoke U et al (1998) In: Proceedings of NACE CORROSION/1998, no. 46
4. Videm K, Dugstad A (1989) Mater Perform 28:63
5. Han J, Nešić S, Brown (2010) Corrosion 66:095003-1–095003-12
6. Han J, Brown BN, Young D et al (2010) J Appl Electrochem 40:683
7. Xia Z, Chou KC, Szklarska-Smialowska Z (1989) Corrosion 45:636
8. Sun Y, George K, Nešić S (2003) In: Proceedings of NACE CORROSION/2003, no. 03327
9. Schmitt G, Gudde T, Strobel-Effertz E (1996) In: Proceedings of NACE CORROSION/1996, no. 9
10. Han J, Young D, Colijn H et al (2009) Ind Eng Chem Res 48:6296
11. Nyborg R, Dugstad A (1998) In: Proceedings of NACE CORROSION/1998, no. 29
12. Chen CF, Lu MX, Sun DB et al (2005) Corrosion 61:594
13. Han J, Nešić S, Yang Y et al (2011) Electrochim Acta 56:5396
14. Bénézeth P, Dandur JL, Harrichoury JC (2009) Chem Geol 265:3
15. Han J, Carey JW, Zhang J (2011) Int J Greenh Gas Control. doi: 10.1016/j.ijggc.2011.02.005
16. Nešić S, Postlethwaite J, Olsen S (1996) Corrosion 52:280
17. Jones DA (1996) Principles and prevention of corrosion, 2nd edn. Prentice Hall, Inc., Upper Saddle River